Expert Systems with Applications 41 (2014) 7466–7477

Contents lists available at ScienceDirect

Expert Systems with Applications

journal homepage: www.elsevier.com/locate/eswa

Gait modification and optimization using neural network–genetic algorithm approach: Application to knee rehabilitation

Marzieh M. Ardestani [a,*], Mehran Moazen [b], Zhongmin Jin [a,c]

[a] State Key Laboratory for Manufacturing System Engineering, School of Mechanical Engineering, Xi'an Jiao tong University, 710054 Xi'an, Shaanxi, China
[b] Medical and Biological Engineering, School of Engineering, University of Hull, Hull, UK
[c] Institute of Medical and Biological Engineering, School of Mechanical Engineering, University of Leeds, Leeds LS2 9JT, UK

ARTICLE INFO

Article history:
Available online 22 June 2014

Keywords:
Gait modification
Tibiofemoral knee joint
Time delay neural network
Genetic algorithm
Contact pressure

ABSTRACT

Gait modification strategies play an important role in the overall success of total knee arthroplasty. There are a number of studies based on multi-body dynamic (MBD) analysis that have minimized knee adduction moment to offload knee joint. Reducing the knee adduction moment, without consideration of the actual contact pressure, has its own limitations. Moreover, MBD-based framework that mainly relies on iterative trial-and-error analysis, is fairly time consuming. This study embedded a time-delay neural network (TDNN) in a genetic algorithm (GA) as a cost effective computational framework to minimize contact pressure. Multi-body dynamic and finite element analyses were performed to calculate gait kinematics/kinetics and the resultant contact pressure for a number of experimental gait trials. A TDNN was trained to learn the nonlinear relation between gait parameters (inputs) and contact pressures (output). The trained network was then served as a real-time cost function in a GA-based global optimization to calculate contact pressure associated with each potential gait pattern. Two optimization problems were solved: first, knee flexion angle was bounded within the normal patterns and second, knee flexion angle was allowed to be increased beyond the normal walking. Designed gait patterns were evaluated through multi-body dynamic and finite element analyses.

The TDNN-GA resulted in realistic gait patterns, compared to literature, which could effectively reduce contact pressure at the medial tibiofemoral knee joint. The first optimized gait pattern reduced the knee contact pressure by up to 21% through modifying the adjacent joint kinematics whilst knee flexion was preserved within normal walking. The second optimized gait pattern achieved a more effective pressure reduction (25%) through a slight increase in the knee flexion at the cost of considerable increase in the ankle joint forces. The proposed approach is a cost-effective computational technique that can be used to design a variety of rehabilitation strategies for different joint replacement with multiple objectives.

1. Introduction

Following total knee arthroplasty (TKA), rehabilitation strategies are of significant importance to accelerate patient recovery (Isaac et al., 2005; Klein, Levine, & Hartzband, 2008), reinforce joint functionality (Moffet et al., 2004; Rahmann, Brauer, & Nitz, 2009), decrease gait asymmetry (Zeni, Mcclelland, & Snyder-Mackler, 2011), and augment the durability and life time of knee prostheses (Fransen, 2011; Mont et al., 2006). Gait rehabilitations mainly aim to decrease knee joint loading through minor changes in human gait patterns. However, recognizing the synergistic kinematic changes, required for joint offloading, is a challenging task, hence; computational approaches have been used to facilitate the design procedure. To best of our knowledge, most of the current literature on gait modification strategies have been designed through multi-body dynamic (MBD) analysis (Ackermann & van den Bogert, 2010; Anderson & Pandy, 2001; Barrios, Crossley, & Davis, 2010; Barrios & Davis, 2007; Fregly, D'Lima, & Colwell, 2009; Fregly, Reinbolt, Rooney, Mitchell, & Chmielewski, 2007; Hunt et al., 2008; Mündermann, Asay, Mündermann, & Andriacchi, 2008; Willson, Torry, Decker, Kernozek, & Steadman, 2001). However, iterative "trial-and-error" MBD analysis, that has been performed in such studies, is fairly time demanding which limits the applicability and generality of the method. Hence, a cost-effective computational framework that minimizes the computational cost is of particular interest.

Besides the computational cost, there are a number of aspects that have not been well addressed by the conventional MBD-based framework. *First*, MBD-based approach attempts to reduce the

* Corresponding author. Tel.: +86 029 83395122.
E-mail address: mostafavizadeh@yahoo.com (M.M. Ardestani).

http://dx.doi.org/10.1016/j.eswa.2014.06.034
0957-4174/

peak values of knee adduction moment (KAM) which is not always a reliable measure since decreasing KAM may not necessarily decrease knee joint loading (Walter, D'Lima, Colwell, & Fregly, 2010); and the results of such approach are sensitive to the chosen reference frame (e.g. laboratory, floating reference frames) (Lin, Lai, Chou, & Ho, 2001; Shull et al., 2012). *Second*, joint-offloading gait patterns are likely to decrease the contact area of articulating surfaces that unfavorably may increase the contact pressure at the knee joint (D'Lima et al., 2008). Therefore, reducing the contact pressure should be concerned as the principal goal of rehabilitation design. Conventional computational frameworks however are inherently unable to consider the contact pressure in the design procedure since the conventional methods require an explicit cost function whilst the relation between gait kinematics and the resultant contact pressure has not been stated explicitly before. Also, predicting the contact pressure requires implementing finite element analysis (FEA) which in turn increases the computational cost (Halloran, Ackermann, Erdemir, & van den Bogert, 2010). A cost-effective surrogate which releases the necessity of iterative FEA is therefore of significant advantage. *Third,* previous studies could not reach a general consensus about the contribution of knee flexion to the knee joint offloading. Knee flexion is a key synergetic parameter that is often increased within the clinical execution of the rehabilitation patterns (Barrios et al., 2010; Fregly et al., 2007; Van Den Noort, Schaffers, Snijders, & Harlaar, 2013). Several studies concluded that increasing the knee flexion would reduce KAM (Fregly, 2008; Fregly, D'Lima, & Colwell, 2009; Fregly et al., 2007), whilst others showed that it has no association with KAM (Creaby, Hunt, Hinman, & Bennell, 2013) or may even increase contact pressure at the knee bearing surfaces (D'Lima et al., 2008). A systematic investigation is required to enhance our understanding of the contribution of knee flexion to the knee joint offloading.

Artificial neural networks (ANN) and genetic algorithm (GA) are two relatively new techniques in the field of biomechanics. Artificial neural network (ANN) can be used as a real-time surrogate model with the ability to *learn* a nonlinear relationship. Once a set of inputs and corresponding outputs are presented to the network, it will then "learn" the causal interactions between inputs and outputs. Given a new set of inputs, the trained neural network (surrogate model) can generalize the relationship to produce the associated outputs. The ANN surrogate therefore can be of significant advantage especially when the original model necessitates repeating a time-consuming computation. For example, ANN has been widely used as a surrogate of FEA (Campoli, Weinans, & Zadpoor, 2012; Hambli, 2010; Hambli, 2011; Lu, Pulasani, Derakhshani, & Guess, 2013; Naito & Torii, 2005; Simic, Hinman, Wrigley, Bennell, & Hunt, 2011; Zadpoor, Campoli, & Weinans, 2013). Genetic algorithm is a time-efficient global optimization technique which searches the entire data space to find the best solution (Goldberg, 1989). In each iteration, only potential candidates that better optimize the cost function will survive to the next iteration. Thus, regardless of the initial point, the search data space is iteratively modified and GA will rapidly converge to the global optimum solution. This in turn assures the robustness of the method and minimizes the computational effort required to find the best solution. Moreover, GA is capable of dealing with multivariable data space, nonlinear input–output interactions and non-explicit, non-differential cost function.

Therefore, the overall aim of this study was to develop a hybrid framework of time delay neural network (TDNN) and genetic algorithm (GA) to address the aforementioned limitations of the literature. In particular this study aimed to (1) optimize the gait pattern in order to minimize the contact pressure at the knee articulating surfaces and (2) investigate the role of knee flexion in knee joint offloading. The advantage of the proposed approach was also compared over the existing knee rehabilitations in the literature.

2. Materials and methods

The proposed computational approach was implemented in the following steps:

Step (1) Experimental gait analysis data were obtained from the literature (Section 2.1), and imported into MBD analysis to calculate gait kinematics and kinetics (Section 2.2). Knee flexion angle and three dimensional knee joint loadings were predicted by MBD, and then served as boundary condition and loading profiles for the finite element simulation to calculate contact pressure (Section 2.3). Gait trials were then outlined via a number of kinematic features and the corresponding maximum contact pressure values (CPRESS-max) (Section 2.4).
Step (2) A time-delay neural network (TDNN) was trained to learn the nonlinear relationship between kinematic features as inputs and the corresponding CPRESS-max values as output (Section2.5).
Step (3) A genetic algorithm (GA) was implemented to search for the optimum kinematic features (optimization variables) which minimized the CPRESS-max at the knee joint bearing surfaces. In this GA, the trained TDNN was served as a real-time cost function to calculate the objective value (CPRESS-max) (Section 2.6).

2.1. Experimental gait data

Experimental gait analysis data of a single subject with unilateral TKA (female, height 167 cm, mass 78.4 kg) was obtained from the literature (https://simtk.org/home/kneeloads; accessed on June 2013). The subject walked with a variety of different gait patterns including *normal*, *medial thrust*, *trunk sway*, *walking pole*, *bouncy*, *crouch*, *smooth* and *fore foot strike*. *Medial thrust*, *trunk sway* and *walking pole* were knee rehabilitation strategies, designed to decrease KAM, whilst the remaining gait trials were different walking patterns to cover the span of executable gait for the subject. Compared to *normal* walking, the subject walked with a slightly decreased pelvis obliquity, slightly increased pelvis axial rotation and leg flexion to implement *medial thrust* pattern. For *trunk sway* pattern, the subject walked with an increased lateral leaning of the trunk in the frontal plane over the standing leg. In *walking pole*, the subject used bilateral poles as walking aids. For each gait pattern, five gait trials were repeated under the same walking condition at a self-selected pace. A total of two complete gait cycles were picked up from each trial, leading to a total of 84 data sets. For further details, see Fregly et al. (2012). Gait trials were recorded in terms of marker trajectory data (Motion Analysis Corp., Santa Rosa, CA) and ground reaction forces (AMTI Corp., Watertown, MA).

2.2. Multi-body dynamic

Experimental ground reaction forces and marker trajectories were imported into the three-dimensional multi-body dynamic simulation software, AnyBody Modeling System (version 5.2, AnyBody Technology, Aalborg, Denmark). A lower extremity musculoskeletal model was used in AnyBody software based on the University of Twente Lower Extremity Model (TLEM) (Klein Horsman, 2007). This model, available in the AnyBody published repository, had 160 muscle units as well as foot, thigh, patella, shank, trunk and thorax segments. Hip joint was modeled as a spherical joint with three degrees of freedom (DOF): flexion–extension, abduction–adduction and internal-external rotation. Knee joint was modeled as a hinge joint with only one DOF for flexion–extension and universal joint was considered for ankle-subtalar complex. Since the assumptions of the simplified knee joint and rigid

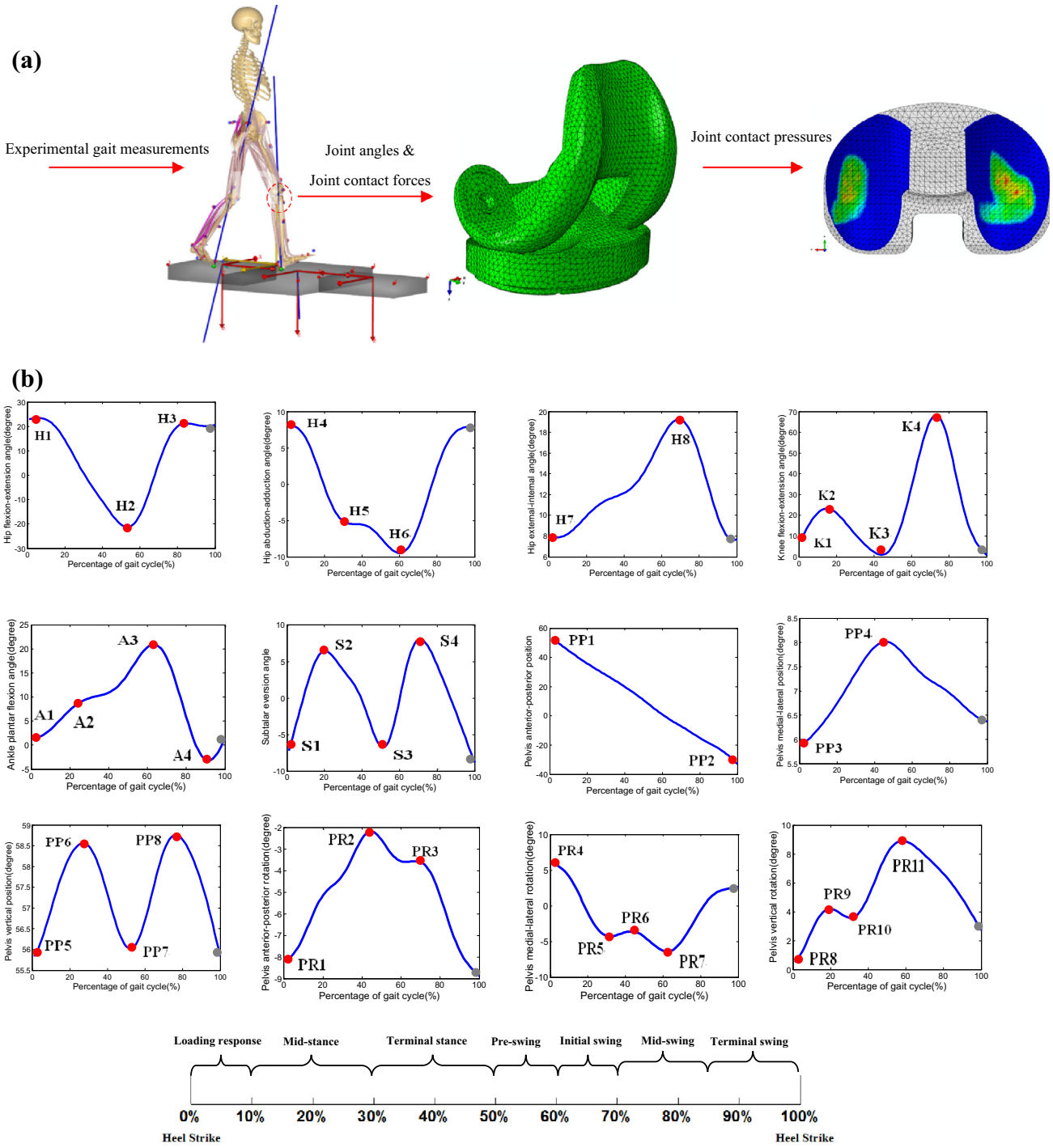

Fig. 1. (a) Experimental gait measurements were imported into multi-body dynamics analysis to calculate joint kinematics/kinetics which were then used by finite element analysis to calculate contact pressure (b) joint angles were parameterized by extremum features (red circles). Due to the periodicity of the gait, joint angle values at the end of the gait cycle (gray points) were equal to the initial values at 0% of the gait cycle except for pelvis position. (For interpretation anterior–posterior of the references to color in this figure legend, the reader is referred to the web version of this article.)

multi-bodies were made, the detailed knee implant was not considered in the MBD analysis. Knee flexion angle and three dimensional knee joint loads, aligned in medial–lateral, proximal–distal and anterior–posterior directions, were calculated for each complete gait cycle. A complete gait cycle was defined as the time period from heel strike of one leg to the following heel strike of the same leg (Vaughan, Davis, & O'Connor, 1992). Computations were then normalized to 100 samples to represent one complete gait cycle. Knee flexion and three dimensional knee joint loads then served as the boundary condition and load profiles for FEA.

2.3. Finite element method

A typical tibiofemoral knee implant was modeled in the commercial finite element package; ABAQUS/Explicit (version 6.12 Simulia Inc., Providence, RI) using the computer aided design (CAD) of a clinically available fixed bearing knee implant. The knee implant consisted of two main parts; femoral component and tibia insert. Rigid body assumptions were applied to both parts, with a simple linear elastic foundation model defined between the two contacting bodies (Halloran, Petrella, & Rullkoetter, 2005). Tetrahedral

Table 1
Description of gait kinematic features.

Joint	Kinematic feature	Description
Hip	H1	Hip flexion at initial contact
Hip	H2	Maximum hip extension at stance
Hip	H3	Maximum hip flexion at swing phase
Hip	H4	Hip abduction at initial contact
Hip	H5	Maximum hip adduction at midstance phase
Hip	H6	Maximum hip adduction at stance phase
Hip	H7	Hip external rotation at initial contact
Hip	H8	Maximum hip internal rotation at swing phase
Knee	K1	Knee flexion at initial contact
Knee	K2	Maximum knee flexion at stance
Knee	K3	Maximum knee extension at stance
Knee	K4	Maximum knee flexion at swing phase
Ankle	A1	Ankle flexion at initial contact
Ankle	A2	Maximum ankle dorsiflexion at midstance
Ankle	A3	Maximum ankle dorsiflexion at stance
Ankle	A4	Maximum ankle plantar flexion at swing phase
Subtalar	S1	Subtalar inversion at initial contact
Subtalar	S2	Maximum subtalar eversion at stance
Subtalar	S3	Maximum subtalar inversion at stance
Subtalar	S4	Maximum subtalar eversion at swing
Pelvis	PP1	Maximum posterior tilt of pelvis
Pelvis	PP2	Maximum anterior tilt of the pelvis
Pelvis	PP3	Maximum lateral obliquity of the pelvis
Pelvis	PP4	Maximum medial obliquity of the pelvis
Pelvis	PP5	Pelvis vertical position at initial contact
Pelvis	PP6	Maximum pelvis upward position at stance
Pelvis	PP7	Maximum pelvis downward position at stance
Pelvis	PP8	Maximum pelvis upward position at swing
Pelvis	PR1	Pelvis anterior rotation at initial contact
Pelvis	PR2	Maximum pelvis posterior rotation at stance
Pelvis	PR3	Maximum pelvis posterior rotation at swing
Pelvis	PR4	Pelvis medial rotation at initial contact
Pelvis	PR5	Maximum pelvis lateral rotation at stance
Pelvis	PR6	Maximum pelvis medial rotation at stance
Pelvis	PR7	Maximum pelvis lateral rotation at swing
Pelvis	PR8	Pelvis axial rotation at initial contact
Pelvis	PR9	Maximum pelvis axial rotation to the left at stance
Pelvis	PR10	Minimum pelvis axial rotation to the right at stance
Pelvis	PR11	Maximum pelvis axial rotation to the left at swing

(C3D10M) elements were used to mesh the model in ABAQUS. Convergence was tested by decreasing the element size from 8 to 0.5 mm in five steps (8, 4, 2, 1, and 0.5 mm). The solution converged on contact pressure (⩽5%) with over 86,000 and 44,000 elements representing the femoral component and the tibia insert respectively. This was also consistent with the previous mesh convergence studies for similar finite element models (Abdelgaied et al., 2011; Halloran et al., 2005). The physical interaction between femoral component and tibia insert was taken into account as a surface-to-surface contact (femur as the master surface and tibia as the slave surface) through a penalty-based approach with an isotropic friction coefficient of 0.04 (Abdelgaied et al., 2011; Halloran et al., 2005). The tibia insert was constrained in all available DOFs and the femoral component was only allowed for flexion–extension under the three dimensional load which were obtained from MBD analysis. The model calculated the contact pressure at each node for each time increment. An output field was created over all simulation frames to compute the maximum value of the contact pressures (CPRESS_max) over the entire gait cycle. Since the medial compartment experiences the CPRESS-max value (Schipplein & Andriacchi, 1991), this part was considered for the rest of the study (Fig. 1a).

Table 2
Genetic algorithm settings in MATLAB.

Genetic algorithm parameter	Value
Population size	50
Scaling function	Rank
Selection function	Tournament
Elite count	2
Crossover fraction	0.85
Crossover function	Single point
Mutation function	Adaptive feasible
Maximum number of generations	100

2.4. Feature extraction

During a complete gait cycle, the extent to which a joint can be moved (range of motion) and the corresponding absolute values of motions directly affect the quality of human gait and joint loading. For example, increasing the "*maximum*" value of hip adduction angle or hip internal rotation would decrease the "*peak*" values of KAM (Barrios et al., 2010). On the other hand, to design a realistic gait modification strategy, the overall trend of kinematic patterns cannot differ significantly from natural human walking habitudes; otherwise the pattern would not be acceptable and executable by the patient. Thus, only the key features of kinematic waveforms are needed to be modified whilst the overall trends should be preserved consistent. Gait kinematics were therefore outlined through a total of 39 descriptive kinematic features (Table 1 and Fig. 1b). These features have been suggested in the literature for a number of studies such as gait analysis (Collins, Ghoussayni, Ewins, & Kent, 2009; Gates, Dingwell, Scott, Sinitski, & Wilken, 2012; Gates, Wilken, Scott, Sinitski, & Dingwell, 2012), gait classification

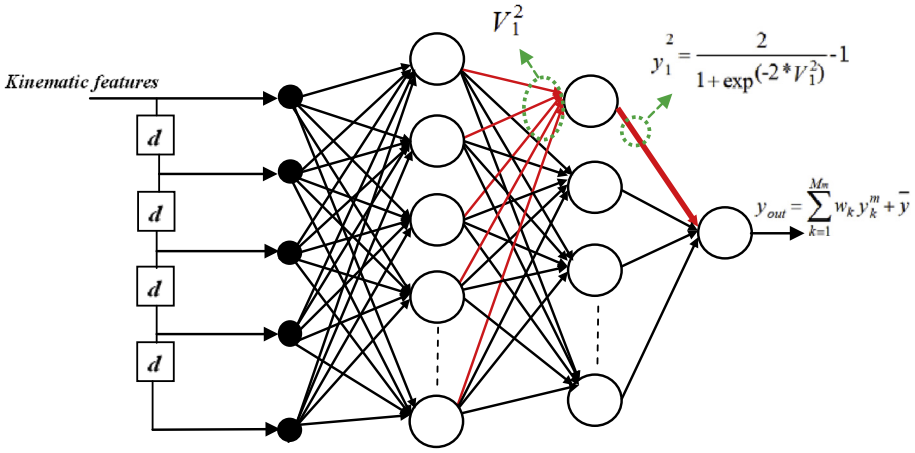

Fig. 2. A schematic diagram of a four-layer TDNN used in this study. The network calculated the maximum values of contact pressure (output) based on gait features (inputs).

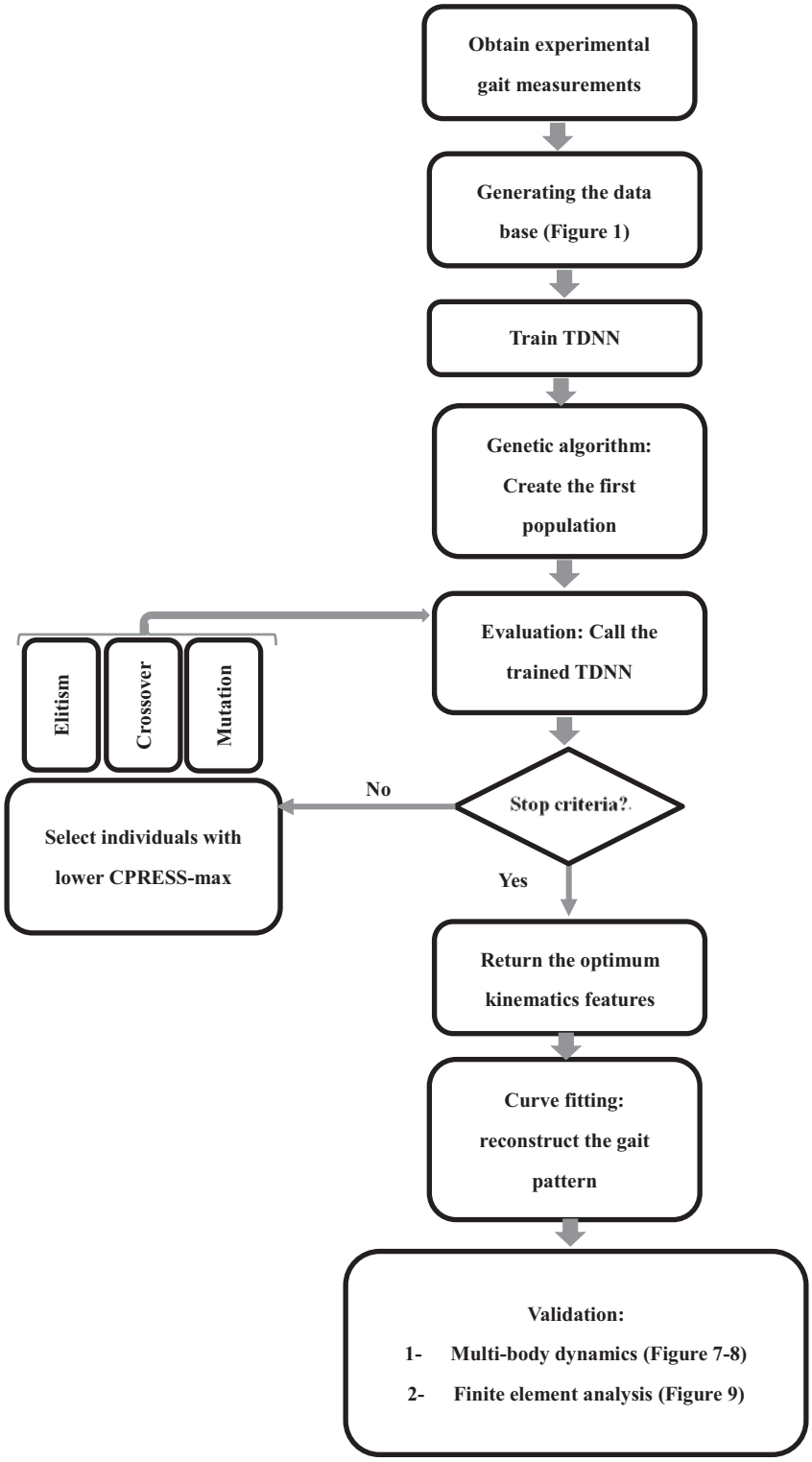

Fig. 3. The flowchart of the proposed TDNNGA.

(Armand, Watelain, Mercier, Lensel, & Lepoutre, 2006), evaluation of joint loading (Simonsen, Moesby, Hansen, Comins, & Alkjaer, 2010), and joint inter-coordination (Wang et al., 2009). Kinematic features (optimization variables) were then allowed to vary within the corresponding ranges of experimental values plus ±20% variations to cover a thorough span of executable movement patterns for the subject. Contact pressure was also characterized by the maximum pressure value occurred over the entire gait cycle (CPRESS-max).

2.5. Time-delay neural network

Time delay neural network (TDNN) was implemented to model the highly nonlinear relationship between kinematic features (39 inputs) and CPRESS-max values (one output). The trained network was then embedded in an optimization process (GA) as a real-time cost function to calculate the objective values (CPRESS-max). The TDNN architecture consisted of a feed forward neural network in which a tapped delay line was added to the input layer (Fig. 2).

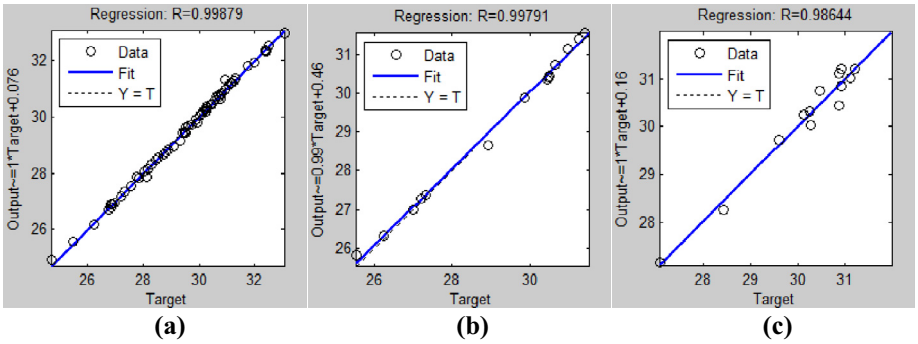

Fig. 4. Network predictions vs. actual CPRESS-max values for (a) train (b) validation and (c) test subsets.

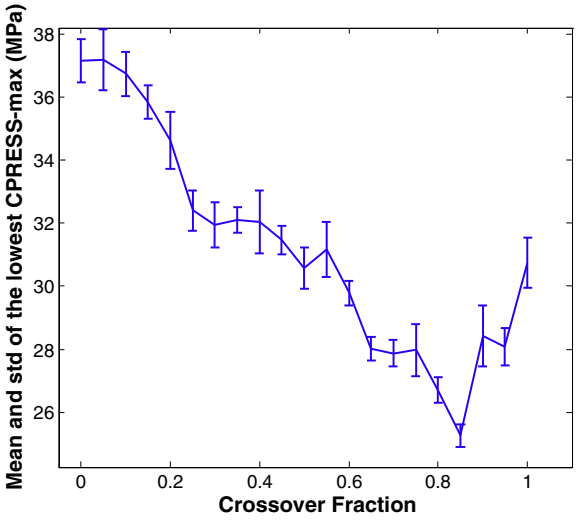

Fig. 5. Mean and standard deviation of the optimized CPRESS-max for different values of crossover fraction in the GA process.

Similar to other types of neural networks, a number of processor units (neurons) were arranged in a certain configuration (layers). A weighted sum of all inputs was fed into each hidden neuron where an activation function acted on this weighted sum to produce the output of the hidden neuron. All of the hidden neurons were activated using "hyperbolic tangent sigmoid" function which linearly scaled its input signal to $[-1,1]$ interval:

$$y_j^m = \frac{2}{1+\exp^{(-2*V_j^m)}} - 1 \quad j = 1,2,\ldots,M_m \tag{1}$$

where y_j^m is the output of jth hidden neuron located at the mth hidden layer, M_m is the number of hidden neurons at the mth hidden layer, and $V_j^m(n)$ is the weighted sum of the signals from the previous layer which was fed to the jth hidden neuron of mth hidden layer:

$$V_j^m = \sum_{k=1}^{Mm-1} (y_k^{m-1} * W_{jk}) + b_j \quad j = 1,2,\ldots,M_m, \quad k = 1,2,\ldots,M_{m-1} \tag{2}$$

where W_{jk} is the weight relating the output of kth neuron located at the $(m-1)$th layer (y_k^{m-1}) to the jth hidden neuron at the mth hidden layer with the bias value of b_j, and M_m and M_{m-1} are the number of neurons at the mth and $(m-1)$th layers respectively. A weighted sum of all hidden neurons' outputs was also fed into the single output node which was activated by a "pure line" function:

$$y_{out} = \sum_{k=1}^{Mm} w_k y_k^m + \bar{y} \tag{3}$$

in which $\bar{y}$ is the output bias.

TDNN was trained using the scaled conjugate gradient algorithm (SCG) (Møller, 1993). The available data space, obtained from MBD and FEA, was randomly divided into three main parts: train (70%), validation (15%) and test (15%) subsets. The train and validation subsets were used to train the network whilst the test subset was not included in training. The network prediction error on the validation subset implied how accurate the network has learned the input–output causal relationship (accuracy). On the other hand, the network prediction error on the test subset indicated the extent to which the trained network could generalize this causal relationship for new inputs (generality). Generally speaking, the structure of the FFANN would build a trade-off between "*prediction accuracy*" and "*generality*". Whilst increasing the number of hidden neurons/layers would increase the prediction accuracy, using too many neurons would decrease the generality and increase the test error. The number of hidden layers and hidden neurons were therefore determined according to the network prediction error for the test and validation subsets. The input delay was also determined by trial and error.

2.6. Genetic algorithm

In the present study, gait optimization was stated as follows:

$$\textit{Minimize } Y: Y = U(X) \quad AX \leqslant b, \quad X_L \leqslant X \leqslant X_U \tag{4}$$

where Y is the CPRESS-max, X is the optimization variables (kinematic features), and U is the trained TDNN. Upper and lower bounds of the optimization variables (X_L and X_U) were obtained from the experimental gait trials plus ±20% variations. Matrix A and vector b described the linear inequality constraints in order to control the natural trends of the gait kinematics (Appendix). Genetic algorithm (GA) was used to search for those kinematic features that could minimize CPRESS-max. Kinematic features (optimization variables) were configured as $1*N$ arrays called individuals ($N = 39$). In each iteration, the GA created a population of individuals and then employed the trained TDNN to calculate the resultant CPRESS-max values associated with potential individuals. Those individuals that led to lower CPRESS-max values were assigned a higher survivorship probability to be selected and make the next population. Each individual is indeed a potential solution and each population is a search space of solutions. Accordingly, after passing several iterations, the population (solution search space) evolved toward the optimized individuals.

The first population was initialized with random individuals in which features of gait kinematics were randomly chosen due to X_L and X_U. The next populations were created through selected indi-

viduals by elitism, crossover and mutation operators of GA (Goldberg, 1989). Table 2 summarizes the setting of the proposed GA in MATLAB (v.2009, Genetic Algorithm toolbox). In the present study, two systematic optimizations were performed: *first*, knee flexion was bounded to vary within the *normal* walking. *Second*, the knee flexion was allowed to vary beyond the *normal* walking up to the *medial thrust* pattern. Once the GA converged to the optimum kinematic features, a typical normal gait cycle was adjusted to these optimum features using the curve fitting technique and the optimized gait pattern was reconstructed. Fig. 3 shows schematic of the proposed combined TDNN-GA methodology in this study.

3. Results

3.1. Network training

A four-layer TDNN with four delay units at its input layer, 20 hidden neurons at the first hidden layer and 15 hidden neurons at the second one, was trained using 70% of the generated data base. Then, it was validated and tested with the remaining 30%. Fig. 4 shows the average performance of the proposed network over 100 training and testing repetitions, each time with a random selection of subsets (Iyer & Rhinehart, 1999). According to the results, the TDNN could accurately predict CPRESS-max values for the training, validation and test subsets. Pearson correlation coefficients, between network predictions (Y axis) and real outputs (X axis), were all above $p = 0.98$. Fig. 4a and b show that the network learned the nonlinear interaction of kinematics and contact pressure variables ($p = 0.99$). Fig. 4c shows that the network could predict the CPRESS-max values corresponding to new sets of kinematics which were not included in the training data space ($p = 0.98$).

3.2. Optimization problem

The crossover fraction substantially affects the convergence of GA. Optimization was therefore run for a variety of different values of crossover fraction ranged from 0 to 1 in the step size of 0.05. The crossover fraction of 0.85 led to the lowest CPRESS-max value (see Fig. 5). Thus, this value was adopted for the rest of this study. In the first optimization problem, knee flexion angle was bounded within *normal* walking. The algorithm was terminated after 75 populations due to stall generation criterion, in which the average change of the objective value (CPRESS-max) was less than 10^{-6} (function tolerance) over 50 populations (stall generations). Fig. 6a shows the mean and the best CPRESS-max values associated with each population. After successful convergence of the algorithm, TDNN-GA achieved the lowest CPRESS-max value of 25.58 MPa for the best individual of the last population.

Using curve fitting technique, a typical normal gait cycle was adjusted to the obtained optimum kinematic features and the optimized gait pattern was reconstructed (Fig. 7). The optimized kinematics laid within the experimental gait patterns suggesting that it would be feasible for the subject to execute the optimized pattern. Using multi-body dynamic analysis, the corresponding joint loadings were computed and compared with the span of experimental values (Fig. 8). Results show that lower extremity joints (ankle, knee and hip) underwent realistic loading conditions i.e. within and with similar pattern to the *experimental* gait trials. Particularly, hip joint loading was generally low in the anterior–posterior direction. A general reduction at the anterior–posterior component of knee joint loading and significant reduction at its medial–lateral component around 40–60% of the gait cycle occurred. Moreover,

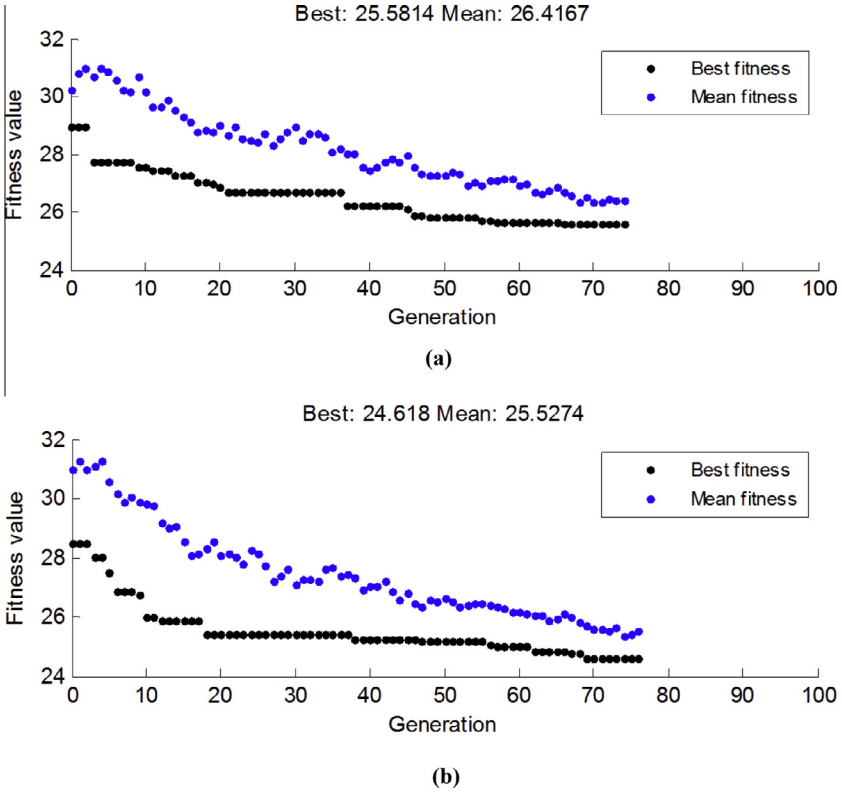

Fig. 6. Convergence of the GA for (a) the first optimization problem in which the knee flexion angle was bounded to normal patterns, (b) the second optimization problem in which the knee flexion angle was allowed to increase beyond normal pattern. "Fitness" refers to the calculated value of CPRESS-max for each individual.

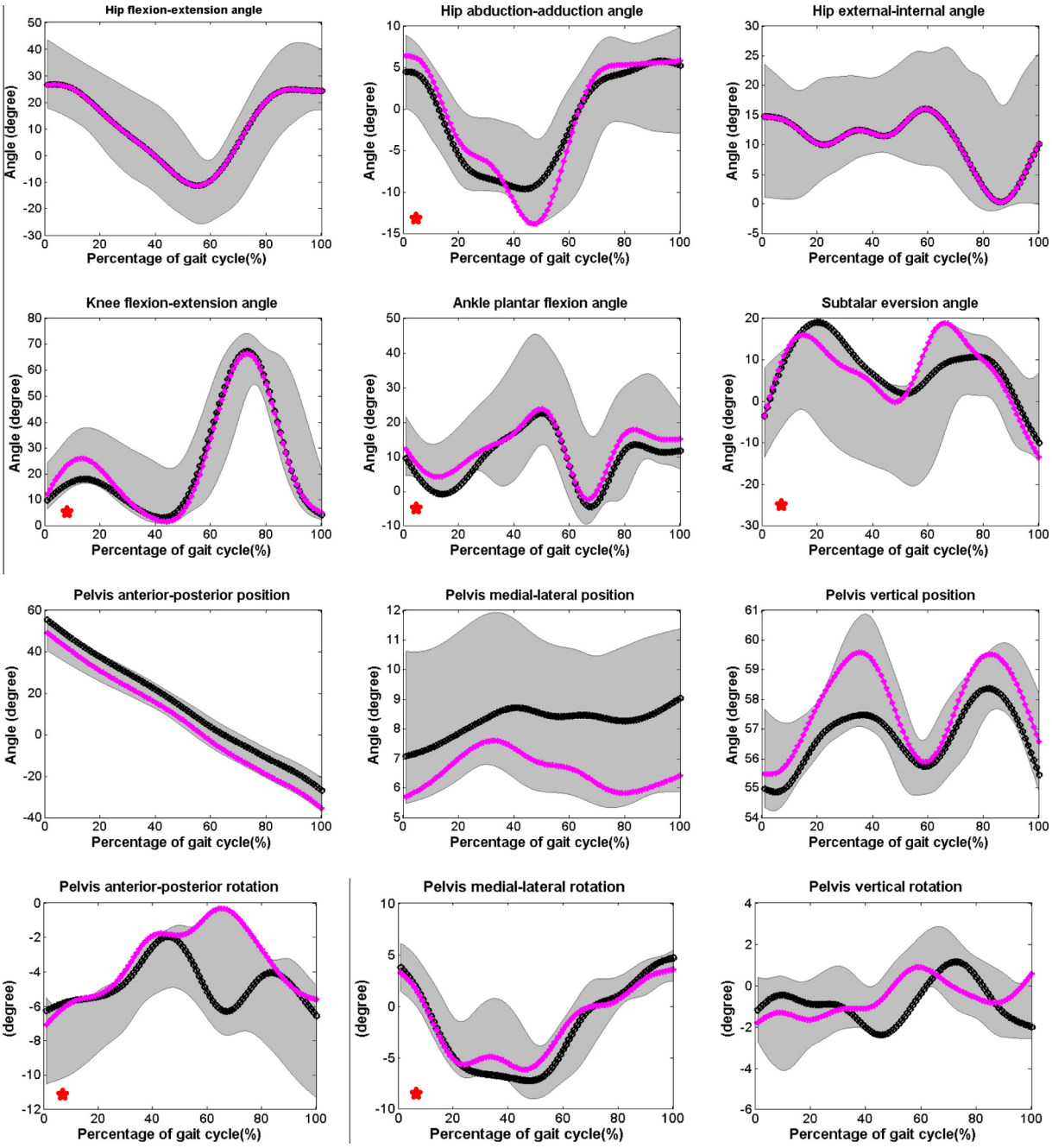

Fig. 7. Kinematics of the first optimized gait pattern (black line) and the second optimized pattern (pink line) laid within the extent of experimental gait trials (gray span). Those kinematics that underwent considerable changes have been marked by ★. (For interpretation of the references to color in this figure legend, the reader is referred to the web version of this article.)

the medial–lateral component of ankle joint loading was significantly decreased accompanied with a reduction at its anterior–posterior component around 40–60% of the gait cycle. Fig. 9 shows the resultant distribution of the maximum contact pressure at the medial tibiofemoral joint over the entire gait cycle. The maximum contact pressure was reduced by 21.8% compared to the *normal* walking, while previously published gait modifications were fairly ineffective to decrease the contact pressure magnitudes.

In the second optimization problem, X_L and X_U were modified and the knee joint flexion was bounded between *normal* and *medial thrust* patterns. The GA achieved the convergence value of 24.61 MPa after 77 populations (Fig. 6b). Reconstructed gait kinematics and the resultant joint loading patterns are presented in Figs. 7 and 8 respectively. Results demonstrate that the second optimized gait pattern also laid within the span of executable gait patterns. The second optimized gait modification led to a significant reduction at the three dimensional hip joint loading (anterior–posterior, proximal–distal and medial–lateral) around 0–25% of the gait cycle. This pattern also led to an overall reduction at anterior–posterior component of the knee joint loading. Anterior–posterior and medial–lateral components of the ankle joint loading were substantially low at 0–25% of the gait cycle, however ankle joint loading was slightly increased around 40–60% of the gait cycle. By comparison, the second optimization problem yielded to a more effective gait modification pattern that better reduced the magnitude of the contact pressure by up to 25% (Fig. 9).

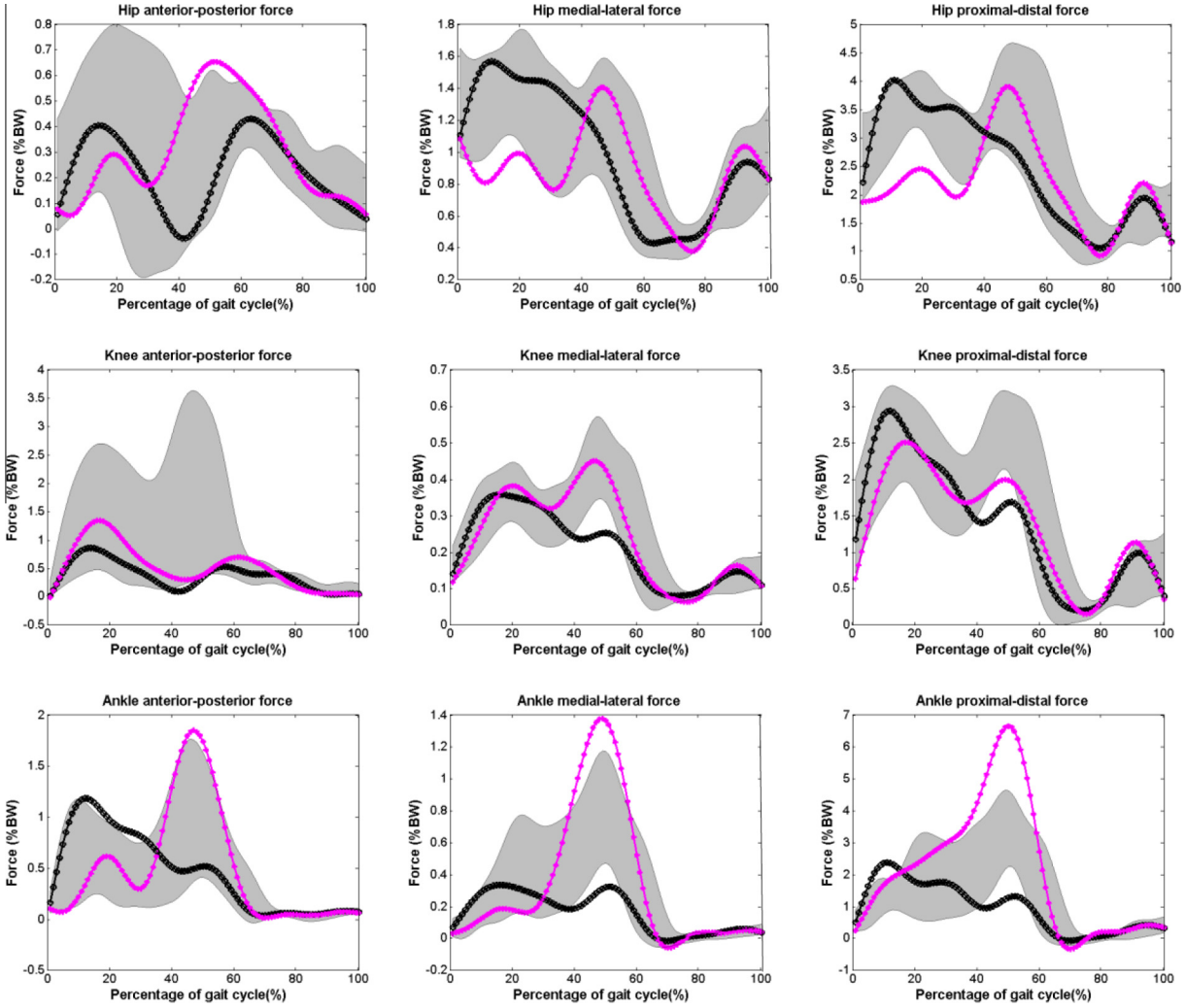

Fig. 8. Resultant joint contact forces of the first optimized gait pattern (black line) and the second optimized pattern (pink line) laid within the extent of experimental gait trials (gray span). (For interpretation of the references to color in this figure legend, the reader is referred to the web version of this article.)

4. Discussion

4.1. Hybrid neural network–genetic algorithm

Neural network was employed: *first*, to model the highly nonlinear relationship between gait kinematics and contact pressure; *second*, to serve as a real-time cost function that allowed the optimization algorithm to be performed in a reasonable computation time. A recent study by Lu et al. (2013) demonstrated that the dynamic structure of a time delay neural network was preferred for modelling the relation between tibiofemoral cartilage load (input) and von Mises stress (output), compared to the traditional static feed forward neural network. Therefore, this structure was used in this study. Moreover, neural network has been used to calculate joint loading from ground reaction forces and gait kinematics (Ardestani et al., 2014a, 2014b) and ground reaction force from gait kinematics (Oh, Choi, & Mun, 2013; Ren, Jones, & Howard, 2008). In this study, neural network was employed to calculate the contact pressure from gait kinematics. The high correlation that was found between the target values and the network predictions for validation and test subsets reassures the reliability of the proposed structure. The TDNN in turn necessitated involving the GA as the optimization technique. In fact, other classical optimization approaches mainly rely on iterative derivation of an explicit cost function however TDNN modeled the problem non-explicitly.

4.2. Current research contribution

There are a number of implications on the gait modification and optimization both in terms of methodology and findings. Major limitations of the previous studies were addressed in the present research. *First,* compared to previous studies in which iterative "trial-and-error" MBD analysis has been used, this study presented a cost-effective computational alternative. TDNN provided a real-time cost function for the GA that could rapidly evaluate the contact pressure associated with each potential gait pattern. Moreover, GA is a stochastic direct search method in which the search data space is modified iteratively. This in turn reduced the computational effort required to find the optimized solution. It should be pointed out that although various gait modifications have been developed in association with knee joint offloading, none of them have yet been accepted as a general modification strategy. In fact, due to the large inter-patient variability, reported in gait kinematics and joint loading patterns (Kutzner et al., 2010; Taylor, Heller, Bergmann, & Duda, 2004), gait rehabilitation strategies should be determined patient specifically. Hence, to design a gait modification strategy, it is crucial that the proposed computational method is cost-effective and easy to recreate.

Second, unlike the previous studies in which KAM reduction has been the principal goal of gait modification, here, contact pressure was adopted as a more accurate criterion for knee joint offloading.

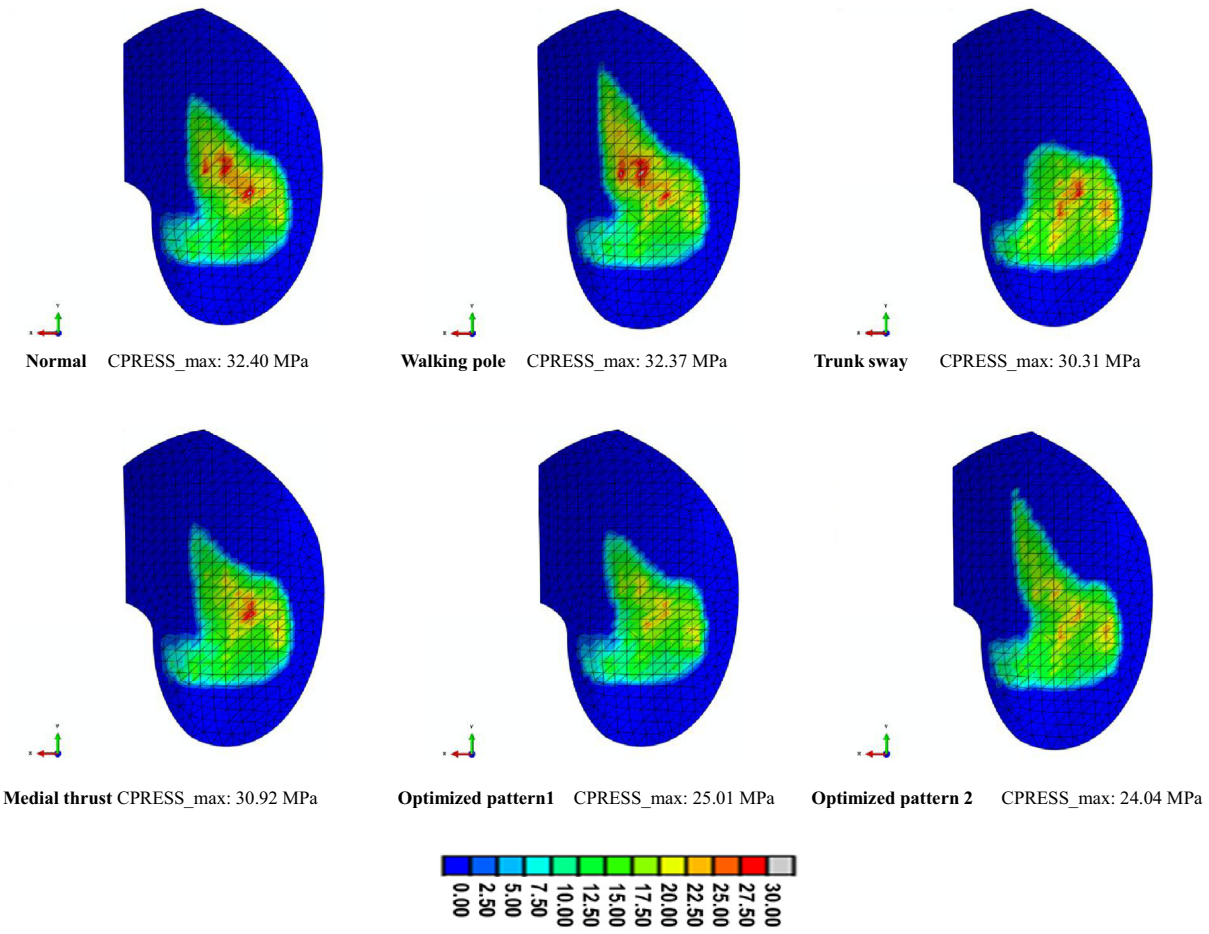

Fig. 9. The resultant maximum values of contact pressures for the optimized gait patterns vs. contact pressures obtained from normal gait and other previously published gait modifications.

This in turn built more confidence in the efficiency of the proposed gait modification. Previous gait modifications were mainly designed to reduce knee joint moment. Although these modification patterns could decrease knee joint loading, none of them could decrease contact pressure at the knee joint bearing surfaces whilst the proposed gait pattern in this study could effectively decrease the contact pressure by up to 25% (see Fig. 9).

Third, whilst previous studies have debated on the influence of increasing knee flexion, this study could address the contribution of knee flexion angle to the knee joint offloading in a systematic manner. Two optimizations were performed: first, knee flexion angle was kept within normal patterns to investigate whether it was possible to decrease knee joint loading through adjacent joints effects. Second, knee flexion was allowed for a non-significant increase. Results showed that in the first optimized gait, contact pressure was reduced by up to 21% whilst knee flexion was preserved within normal walking. In the second optimized pattern, a more effective pressure reduction (25%) was achieved with a slight increase in the knee flexion at the cost of considerable increase in the ankle joint forces at 40–60% of the gait cycle. This observation is consistent with previous studies (Fregly et al., 2007) and suggests that perhaps the first optimization pattern in which joint reaction forces were within the experimental range might be more physiologically feasible. Allowing the knee flexion angle to be more increased led to higher ankle joint loading and a gradual reduction in the contact area which in turn increased contact pressure.

Overall, hip adduction, ankle flexion, subtalar eversion, pelvis posterior rotation and pelvis medial–lateral rotation were increased during the stance phase for both optimized gait patterns (see Fig. 7). However it should be noted that the exact amount of kinematic changes, compared to normal gait, was not reported in this study since specific gait rehabilitation, designed for a particular subject, may not be equally applicable for other patients. Therefore, the quantitative amount of kinematic variations, compared to normal gait, was not focused in this study.

4.3. Limitations

There were several limitations in this study: (1) there was a lack of clinical investigation on the estimated kinematics. Nevertheless, from a technical point of view, the predicted kinematic waveforms are expected to be feasible since the TDNN was trained based on executable walking patterns. Once the network learns this dynamic, it uses this dynamic as the acting function to respond to new sets of inputs. Therefore, it is unlikely that it would generate highly aberrant kinematics. Regardless, further investigations are required to test whether the predicted kinematics is feasible to implement for compensatory or unexpected effects on the other joints or the contra-lateral limb; (2) rigid body constraints were applied to both the femoral and tibia components. Halloran et al. (2005) showed that rigid body analysis of the tibiofemoral knee implant can calculate contact pressure in an acceptable consistence with a full deformable model whilst rigid body analysis would be much more time-efficient. Therefore, in order to produce the training data base, required to train the neural network, rigid body constraints were applied. This was consistent with the present multi-body dynamic

analysis in which no detailed modelling on the knee implant was included; (3) a typical knee implant was adopted in the present study. Although this implant has been widely used in literature (Clayton, Amin, Gaston, & Brenkel, 2006; Dalury, Gonzales, Adams, Gruen, & Trier, 2008; Ranawat et al., 2004; Willing & Kim, 2011), its dimensions were different from the original knee prosthesis by which the subject was implanted. In fact, the subject was implanted with a custom-made sensor-based prosthesis which was specifically produced to measure *in vivo* knee joint loading (Fregly et al., 2012). Accordingly, in this study, a typical commercial knee implant was preferred to test the efficiency of the proposed knee rehabilitation patterns. Nevertheless, the proposed methodology should be equally applicable to other implant geometries and (4) the knee joint was modeled with only one DOF (flexion–extension). Although six DOFs are possible for the knee joint, the dominant movement of the knee joint takes place in the sagittal plane and knee joint has been mostly simplified as a hinge joint, especially for the knee rehabilitation design purposes (Ackermann & van den Bogert, 2010; Anderson & Pandy, 2001; Fregly et al., 2007).

5. Conclusion

A time-delay neural network was embedded in a genetic algorithm to predict a gait pattern that would minimize the contact pressure at the knee joint bearing surfaces. The proposed algorithm suggested an optimum gait pattern in which hip adduction, ankle flexion, subtalar eversion, pelvis posterior rotation and pelvis medial–lateral rotation were slightly increased during the stance phase. Compared to the available gait rehabilitations, the proposed gait pattern could decrease the knee contact pressure by up to 25%. Compared to the conventional MBD-based framework in gait rehabilitation design, the present methodology facilitated a more practical and reliable design procedure at a lower computational cost: (1) instead of using knee adduction moment, contact pressure was considered as a more accurate criterion which led to a more efficient gait modification, (2) using the time-delay neural network, the proposed computational framework was considerably faster and time-efficient. The computational framework therefore can be easily repeated for any given subject. Moreover, (3) the conflicting effect of the knee flexion was addressed through two systematic optimization frameworks: (i) knee joint may be offloaded without any changes in the knee flexion angle (ii) a slight increase in the knee flexion angle might better reduce contact pressure but at the cost of ankle joint over loading and (iii) large increase in the knee flexion angle reduced the contact area and yielded to an increase in the contact pressure.

Various future direction from this study can be considered: (1) on the methodological level, more rigorous tribological metrics (e.g. wear), constraints (e.g. energy expenditure) or gait balance requirements can be included into the computational framework to enhance the predications; (2) on the validation level, further clinical studies are required to validate the finding of such studies; (3) on a wider application level, the proposed methodology in this study has wider implications in design and development of rehabilitation protocols for broader numbers of subjects and other joints such as hip and ankle.

Acknowledgments

This work was supported by "the Fundamental Research Funds for the Central Universities and national Natural Science Foundation of China [E050702, 51323007]". The authors gratefully acknowledge "Grand Challenge Competition to Predict *In Vivo* Knee Loads" for releasing the experimental data. The authors would like to thank Shanghai Gaitech Scientific Instruments Co. Ltd for supplementing AnyBody software used in this study.

Appendix A. Supplementary data

Supplementary data associated with this article can be found, in the online version, at http://dx.doi.org/10.1016/j.eswa.2014.06.034.

References

Abdelgaied, A., Liu, F., Brockett, C., Jennings, L., Fisher, J., & Jin, Z. (2011). Computational wear prediction of artificial knee joints based on a new wear law and formulation. *Journal of Biomechanics, 44*, 1108–1116.

Ackermann, M., & van den Bogert, A. J. (2010). Optimality principles for model-based prediction of human gait. *Journal of Biomechanics, 43*, 1055–1060.

Anderson, F. C., & Pandy, M. G. (2001). Dynamic optimization of human walking. *Transactions-American Society of Mechanical Engineers Journal of Biomechanical Engineering, 123*, 381–390.

Ardestani, M. M., Chen, Z., Wang, L., Lian, Q., Liu, Y., He, J., et al. (2014a). Feed forward artificial neural network to predict contact force at medial knee joint: Application to gait modification. *Neurocomputing, 139*, 114–129.

Ardestani, M. M., Zhang, X., Wang, L., Lian, Q., Liu, Y., He, J., et al. (2014b). Human lower extremity joint moment prediction: A wavelet neural network approach. *Expert Systems with Applications, 41*, 4422–4433.

Armand, S., Watelain, E., Mercier, M., Lensel, G., & Lepoutre, F.-X. (2006). Identification and classification of toe-walkers based on ankle kinematics, using a data-mining method. *Gait & Posture, 23*, 240–248.

Barrios, J. A., Crossley, K. M., & Davis, I. S. (2010). Gait retraining to reduce the knee adduction moment through real-time visual feedback of dynamic knee alignment. *Journal of Biomechanics, 43*, 2208–2213.

Barrios, J. A., & Davis, I. S. (2007). A gait modification to reduce the external adduction moment at the knee: a case study. In *31st annual meeting of the American society of biomechanics*. Stanford, CA, paper.

Campoli, G., Weinans, H., & Zadpoor, A. A. (2012). Computational load estimation of the femur. *Journal of the Mechanical Behavior of Biomedical Materials, 10*, 108–119.

Clayton, R. A., Amin, A. K., Gaston, M. S., & Brenkel, I. J. (2006). Five-year results of the Sigma total knee arthroplasty. *The Knee, 13*, 359–364.

Collins, T. D., Ghoussayni, S. N., Ewins, D. J., & Kent, J. A. (2009). A six degrees-of-freedom marker set for gait analysis: repeatability and comparison with a modified Helen Hayes set. *Gait & Posture, 30*, 173–180.

Creaby, M. W., Hunt, M. A., Hinman, R. S., & Bennell, K. L. (2013). Sagittal plane joint loading is related to knee flexion in osteoarthritic gait. *Clinical Biomechanics, 28*, 916–920.

D'Lima, D. D., Steklov, N., Fregly, B. J., Banks, S. A., & Colwell, C. W. (2008). In vivo contact stresses during activities of daily living after knee arthroplasty. *Journal of Orthopaedic Research, 26*, 1549–1555.

Dalury, D. F., Gonzales, R. A., Adams, M. J., Gruen, T. A., & Trier, K. (2008). Midterm results with the PFC Sigma total knee arthroplasty system. *The Journal of Arthroplasty, 23*, 175–181.

Fransen, M. (2011). *Rehabilitation after knee replacement surgery for osteoarthritis. Seminars in arthritis and rheumatism*. Elsevier, p. 93.

Fregly, B. J. (2008). Computational assessment of combinations of gait modifications for knee osteoarthritis rehabilitation. *IEEE Transactions on Biomedical Engineering, 55*, 2104–2106.

Fregly, B. J., Besier, T. F., Lloyd, D. G., Delp, S. L., Banks, S. A., Pandy, M. G., et al. (2012). Grand challenge competition to predict in vivo knee loads. *Journal of Orthopaedic Research, 30*, 503–513.

Fregly, B. J., D'Lima, D. D., & Colwell, C. W. (2009). Effective gait patterns for offloading the medial compartment of the knee. *Journal of Orthopaedic Research, 27*, 1016–1021.

Fregly, B. J., Reinbolt, J. A., Rooney, K. L., Mitchell, K. H., & Chmielewski, T. L. (2007). Design of patient-specific gait modifications for knee osteoarthritis rehabilitation. *IEEE Transactions on Biomedical Engineering, 54*, 1687–1695.

Gates, D. H., Dingwell, J. B., Scott, S. J., Sinitski, E. H., & Wilken, J. M. (2012). Gait characteristics of individuals with transtibial amputations walking on a destabilizing rock surface. *Gait & Posture, 36*, 33–39.

Gates, D. H., Wilken, J. M., Scott, S. J., Sinitski, E. H., & Dingwell, J. B. (2012). Kinematic strategies for walking across a destabilizing rock surface. *Gait & Posture, 35*, 36–42.

Goldberg, D. (1989). *Genetic algorithms in search, optimization, and machine learning*. Reading, MA: Addison-Wesley.

Halloran, J. P., Ackermann, M., Erdemir, A., & van den Bogert, A. J. (2010). Concurrent musculoskeletal dynamics and finite element analysis predicts altered gait patterns to reduce foot tissue loading. *Journal of Biomechanics, 43*, 2810–2815.

Halloran, J. P., Petrella, A. J., & Rullkoetter, P. J. (2005). Explicit finite element modeling of total knee replacement mechanics. *Journal of Biomechanics, 38*, 323–331.

Hambli, R. (2010). Application of neural networks and finite element computation for multiscale simulation of bone remodeling. *Journal of Biomechanical Engineering, 132*, 114502.

Hambli, R. (2011). Numerical procedure for multiscale bone adaptation prediction based on neural networks and finite element simulation. *Finite Elements in Analysis and Design, 47*, 835–842.

Hunt, M., Birmingham, T., Bryant, D., Jones, I., Giffin, J., Jenkyn, T., et al. (2008). Lateral trunk lean explains variation in dynamic knee joint load in patients with medial compartment knee osteoarthritis. *Osteoarthritis and Cartilage, 16*, 591–599.

Isaac, D., Falode, T., Liu, P., l'Anson, H., Dillow, K., & Gill, P. (2005). Accelerated rehabilitation after total knee replacement. *The Knee, 12*, 346–350.

Iyer, M. S., & Rhinehart, R. R. (1999). A method to determine the required number of neural-network training repetitions. *IEEE Transactions on Neural Networks, 10*, 427–432.

Klein, G. R., Levine, H. B., & Hartzband, M. A. (2008). *Pain management and accelerated rehabilitation after total knee arthroplasty*. Elsevier, pp. 248–251.

Klein Horsman, M. D. (2007). The Twente lower extremity model: Consistent dynamic simulation of the human locomotor apparatus, University of Twente.

Kutzner, I., Heinlein, B., Graichen, F., Bender, A., Rohlmann, A., Halder, A., et al. (2010). Loading of the knee joint during activities of daily living measured *in vivo* in five subjects. *Journal of Biomechanics, 43*, 2164–2173.

Lin, C.-J., Lai, K.-A., Chou, Y.-L., & Ho, C.-S. (2001). The effect of changing the foot progression angle on the knee adduction moment in normal teenagers. *Gait & Posture, 14*, 85–91.

Lu, Y., Pulasani, P. R., Derakhshani, R., & Guess, T. M. (2013). Application of neural networks for the prediction of cartilage stress in a musculoskeletal system. *Biomedical Signal Processing and Control, 8*, 475–482.

Møller, M. F. (1993). A scaled conjugate gradient algorithm for fast supervised learning. *Neural Networks, 6*, 525–533.

Mündermann, A., Asay, J. L., Mündermann, L., & Andriacchi, T. P. (2008). Implications of increased medio-lateral trunk sway for ambulatory mechanics. *Journal of Biomechanics, 41*, 165–170.

Moffet, H., Collet, J.-P., Shapiro, S. H., Paradis, G., Marquis, F., & Roy, L. (2004). Effectiveness of intensive rehabilitation on functional ability and quality of life after first total knee arthroplasty: A single-blind randomized controlled trial. *Archives of Physical Medicine and Rehabilitation, 85*, 546–556.

Mont, M. A., Bonutti, P. M., Seyler, T. M., Plate, J. F., Delanois, R. E., & Kester, M. . *The future of high performance total hip arthroplasty*. *Seminars in arthroplasty*. Elsevier, pp. 88–92.

Naito, K., & Torii, S. (2005). Effects of laterally wedged insoles on knee and subtalar joint moments. *Archives of Physical Medicine and Rehabilitation*, 86.

Oh, S. E., Choi, A., & Mun, J. H. (2013). Prediction of ground reaction forces during gait based on kinematics and a neural network model. *Journal of Biomechanics, 46*, 2372–2380.

Rahmann, A. E., Brauer, S. G., & Nitz, J. C. (2009). A specific inpatient aquatic physiotherapy program improves strength after total hip or knee replacement surgery: A randomized controlled trial. *Archives of Physical Medicine and Rehabilitation, 90*, 745–755.

Ranawat, A. S., Rossi, R., Loreti, I., Rasquinha, V. J., Rodriguez, J. A., & Ranawat, C. S. (2004). Comparison of the PFC Sigma fixed-bearing and rotating-platform total knee arthroplasty in the same patient: short-term results. *The Journal of Arthroplasty, 19*, 35–39.

Ren, L., Jones, R. K., & Howard, D. (2008). Whole body inverse dynamics over a complete gait cycle based only on measured kinematics. *Journal of Biomechanics, 41*, 2750–2759.

Schipplein, O., & Andriacchi, T. (1991). Interaction between active and passive knee stabilizers during level walking. *Journal of Orthopaedic Research, 9*, 113–119.

Shull, P. B., Shultz, R., Silder, A., Dragoo, J. L., Besier, T. F., Cutkosky, M. R., et al. (2012). Toe-in gait reduces the first peak knee adduction moment in patients with medial compartment knee osteoarthritis. *Journal of Biomechanics*.

Simic, M., Hinman, R. S., Wrigley, T. V., Bennell, K. L., & Hunt, M. A. (2011). Gait modification strategies for altering medial knee joint load: A systematic review. *Arthritis Care & Research, 63*, 405–426.

Simonsen, E. B., Moesby, L. M., Hansen, L. D., Comins, J., & Alkjaer, T. (2010). Redistribution of joint moments during walking in patients with drop-foot. *Clinical Biomechanics, 25*, 949–952.

Taylor, W. R., Heller, M. O., Bergmann, G., & Duda, G. N. (2004). Tibio-femoral loading during human gait and stair climbing. *Journal of Orthopaedic Research, 22*, 625–632.

Van Den Noort, J. C., Schaffers, I., Snijders, J., & Harlaar, J. (2013). The effectiveness of voluntary modifications of gait pattern to reduce the knee adduction moment. *Human Movement Science*.

Vaughan, C. L., Davis, B. L., & O'Connor, J. C. (1992). *Dynamics of human gait*. USA: Human Kinetics Publishers.

Walter, J. P., D'Lima, D. D., Colwell, C. W., & Fregly, B. J. (2010). Decreased knee adduction moment does not guarantee decreased medial contact force during gait. *Journal of Orthopaedic Research, 28*, 1348–1354.

Wang, T.-M., Yen, H.-C., Lu, T.-W., Chen, H.-L., Chang, C.-F., Liu, Y.-H., et al. (2009). Bilateral knee osteoarthritis does not affect inter-joint coordination in older adults with gait deviations during obstacle-crossing. *Journal of Biomechanics, 42*, 2349–2356.

Willing, R., & Kim, I. Y. (2011). Design optimization of a total knee replacement for improved constraint and flexion kinematics. *Journal of Biomechanics, 44*, 1014–1020.

Willson, J., Torry, M. R., Decker, M. J., Kernozek, T., & Steadman, J. (2001). Effects of walking poles on lower extremity gait mechanics. *Medicine and Science in Sports and Exercise, 33*, 142–147.

Zadpoor, A. A., Campoli, G., & Weinans, H. (2013). Neural network prediction of load from the morphology of trabecular bone. *Applied Mathematical Modelling, 37*, 5260–5276.

Zeni, J., Jr., Mcclelland, J., & Snyder-Mackler, L. (2011). 193 A novel rehabilitation paradigm to improve movement symmetry and maximize long-term outcomes after total knee arthroplasty. *Osteoarthritis and Cartilage, 19*, S96–S97.